TRAPPC4 regulates the intracellular trafficking of PD-L1 and anti-tumor immunity

Yimeng Ren[#1, 2, 3], Yun Qian[#1, 2, 3], Luoyan Ai[1,2, 3, 4], Yile Xie[1, 2, 3], Yaqi Gao[1, 2, 3], Ziyan Zhuang[1, 2, 3], Jinxian Chen[5], Ying-Xuan Chen[1, 2, 3], Jing-Yuan Fang[*1, 2, 3]

[1] State Key Laboratory for Oncogenes and Related Genes, Key Laboratory of Gastroenterology and Hepatology, Ministry of Health, 145 Middle Shandong Road, 200001 Shanghai, China [2] Division of Gastroenterology and Hepatology, Renji Hospital, School of Medicine, Shanghai Jiao Tong University, 145 Middle Shandong Road, 200001 Shanghai, China [3]Shanghai Institute of Digestive Disease, Renji Hospital, School of Medicine, Shanghai Jiao Tong University, 145 Middle Shandong Road, 200001 Shanghai, China [4] Department of Medical Oncology, Zhongshan Hospital, Fudan University, 180 FengLin Road, 200032, Shanghai, China [5] Division of Gastrointestinal Surgery, Renji Hospital, School of Medicine, Shanghai Jiao Tong University, 145 Middle Shandong Road, 200001 Shanghai, China
[#]Contributed equally.

Supplementary information

Table of Contents

Supplementary Figures

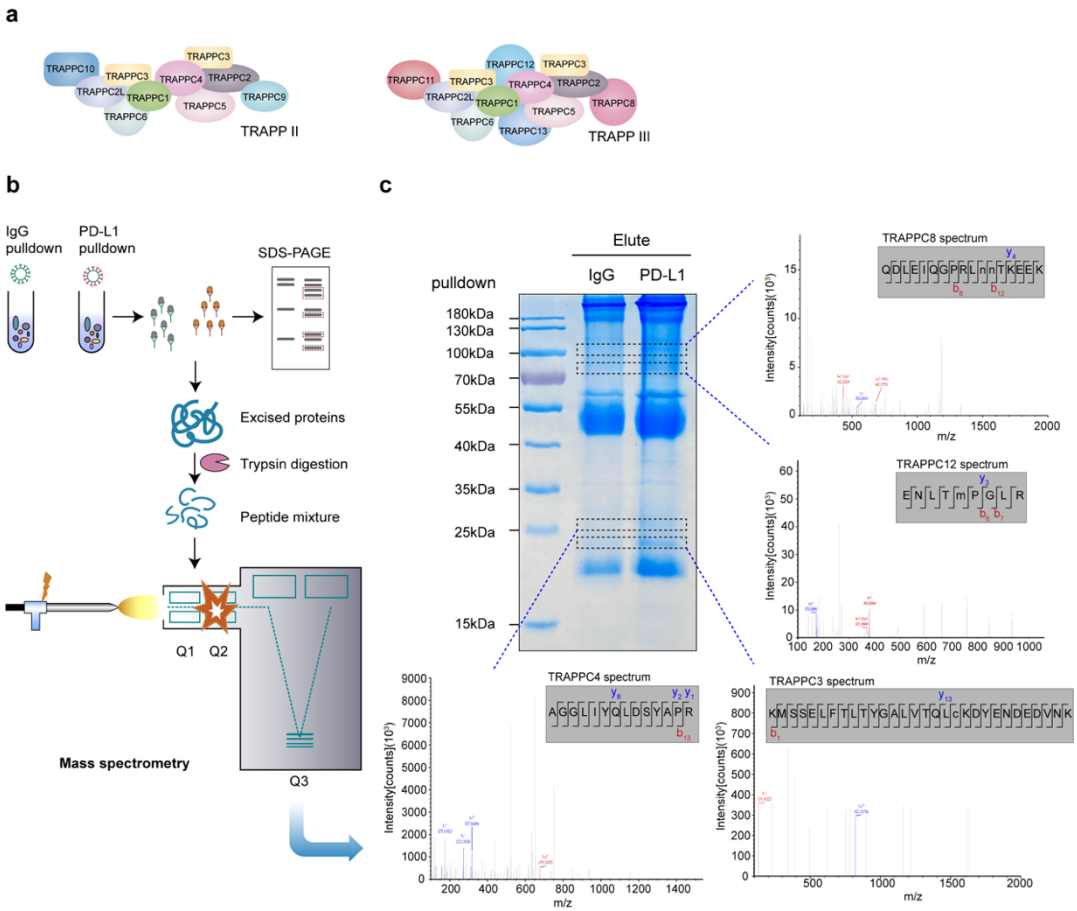

Supplementary Fig. 1 Detection of PD-L1-binding TRAPP subunits by mass spectrometry. a, Model of the mammalian TRAPP complexes. **b**, Schematic representation of the workflow to detect PD-L1-binding TRAPP subunits. The antibody targeting PD-L1 was added into a lysate of RKO cells to immunoprecipitated the endogenous PD-L1 protein along with its interacting proteins. Immunoprecipitation of IgG was included as the negative control. The proteins were separated by SDS-PAGE and stained by Coomassie brilliant blue to determine the specific stained bands in PD-L1 immunoprecipitation and analyzed using LC-MS/MS. **c**, Mass spectrometry analysis identified TRAPPC3, 4, 8, and 12 as the interaction partners of PD-L1. The bands indicated in this figure were analyzed using LC-MS/MS and the interacting TRAPP subunits were identified in presence of PD-L1 immunoprecipitation and absence of that of IgG. Source data are provided as a Source Data file.

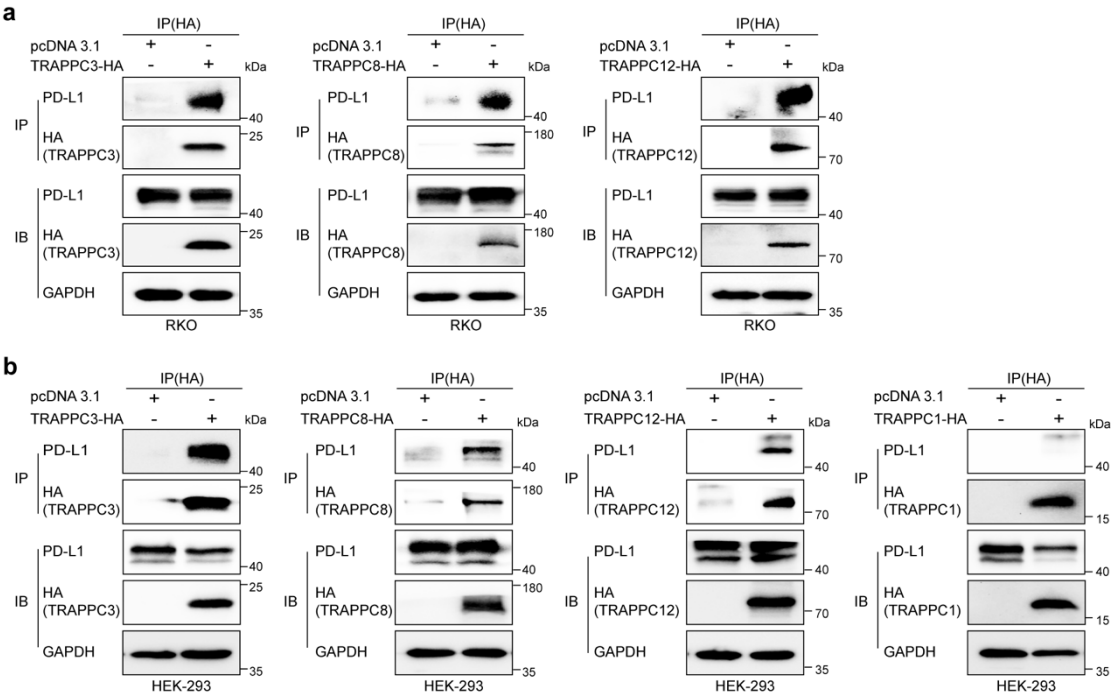

Supplementary Fig. 2 Verification of the results of the mass spectrometry in RKO and HEK-293 cells. a& b, The results of the mass spectrometry were verified by immunoprecipitation of the indicated TRAPP subunits in RKO (**a**) and HEK293 (**b**) cells. RKO and HEK293 cells were transfected with HA-TRAPPC3, 8, and 12 plasmids and immunoprecipitated with anti-HA antibodies to detect their interaction with PD-L1. HA-TRAPPC1 was included as a control representing the TRAPP subunits lacking an interaction with PD-L1. This experiment was repeated twice with similar results. Source data are provided as a Source Data file.

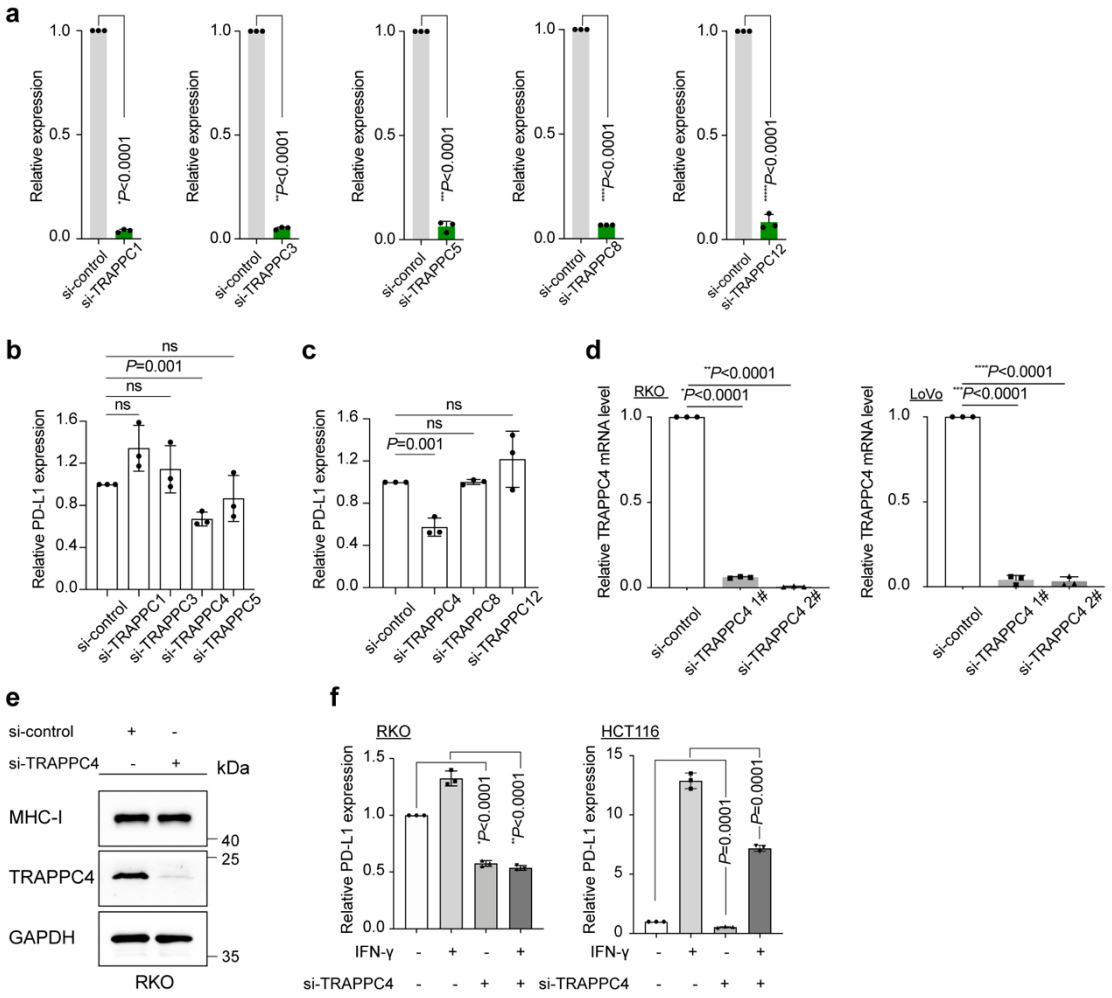

Supplementary Fig. 3 Regulation of PD-L1 expression by subunits of the TRAPP complex. a, The knockdown efficiency of siRNAs targeting different subunits of the TRAPP complex was determined using qRT-PCR in RKO cells. The means ± SD of three biological replicates is shown. ($^{*}P$=2.19e-9, $^{**}P$= 1.1e-9, $^{***}P$=3.69e-7, $^{****}P$=8e-15, $^{*****}P$=1.72e-6) **b& c**, The semiquantitative analysis of the indicated immunoblots in **Fig. 2b**. Values indicated means ± SD of the relative level of PD-L1 from three independent replicates, compared using a two-sided Student's *t* test. **d**, The knockdown efficiency of TRAPPC4 siRNA was determined using qRT-PCR in RKO cells and LoVo cells. The means ± SD of three biological replicates is shown. Data were analyzed by two-sided student's *t* test. ($^{*}P$=3.82e-10, $^{**}P$=6e-11, $^{***}P$=3.79e-7, $^{****}P$=4.13e-7) **e**, Western blot showing that interference with TRAPPC4 expression did not alter the level of MHC class I. The experiment was conducted three times independently with similar results. **f**, Values indicate means ± SD of the relative

gray values of the indicated blots from three independent assays, compared by a two-sided Student's *t* test. ($^{*}P$=7.93e-6, $^{**}P$=3.84e-5) Source data are provided as a Source Data file.

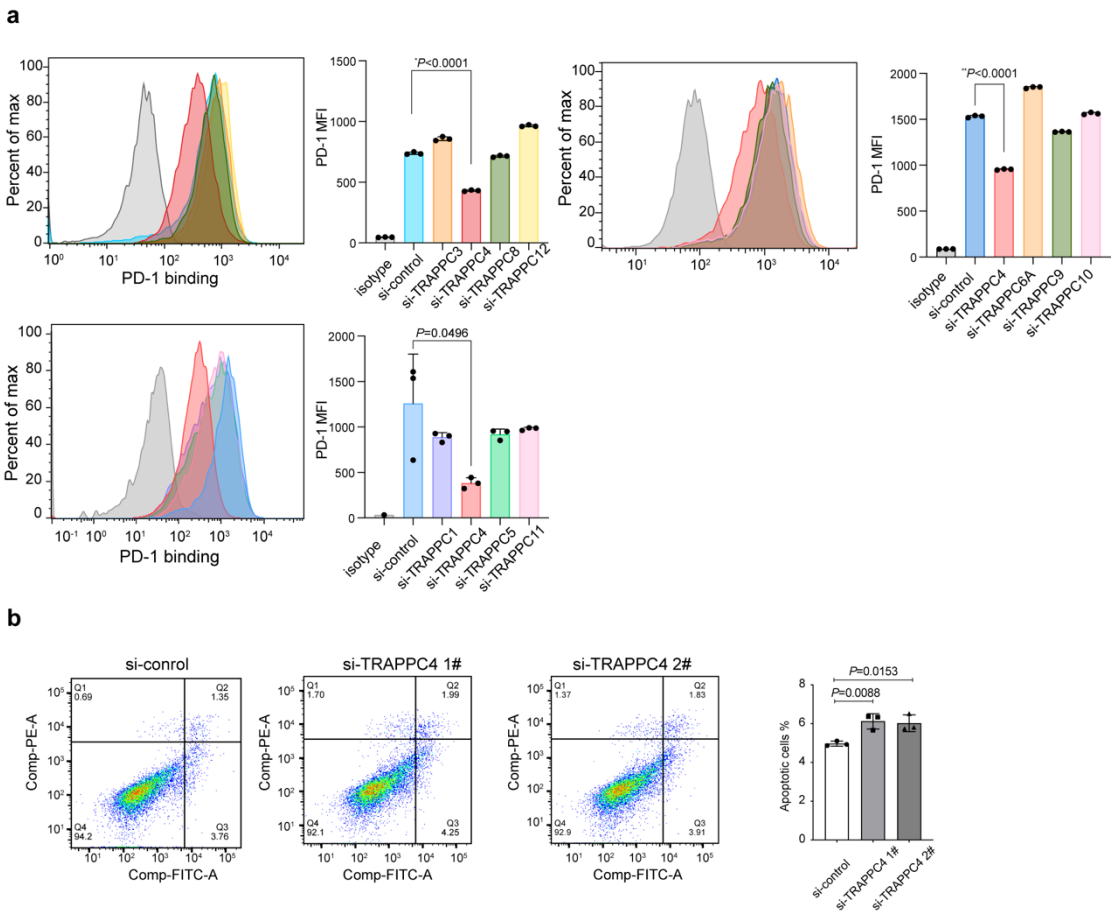

Supplementary Fig. 4 The effects of TRAPPC4 and other TRAPP subunits on anti-tumor immunity. a, The binding of PD-1 with PD-L1 on RKO cells treated with the indicated siRNAs was detected using flow cytometry. The y-axis indicates the MFI of fluorescence conjugated PD-1. This figure represents the result of three independent experimental replicates. Values indicate means ± SD, compared using a two-tailed Student's *t* test. ($^{*}P$=1.57e-6, $^{**}P$=1.77e-7) **b**, Flow cytometry assay indicating that a slight increase in apoptosis was induced by interference with TRAPPC4 expression. Values indicate means ± SD of the percentage of apoptotic cells from three independent replicates. Statistical analysis was performed using a two-tailed Student's *t* test. Source data are provided as a Source Data file.

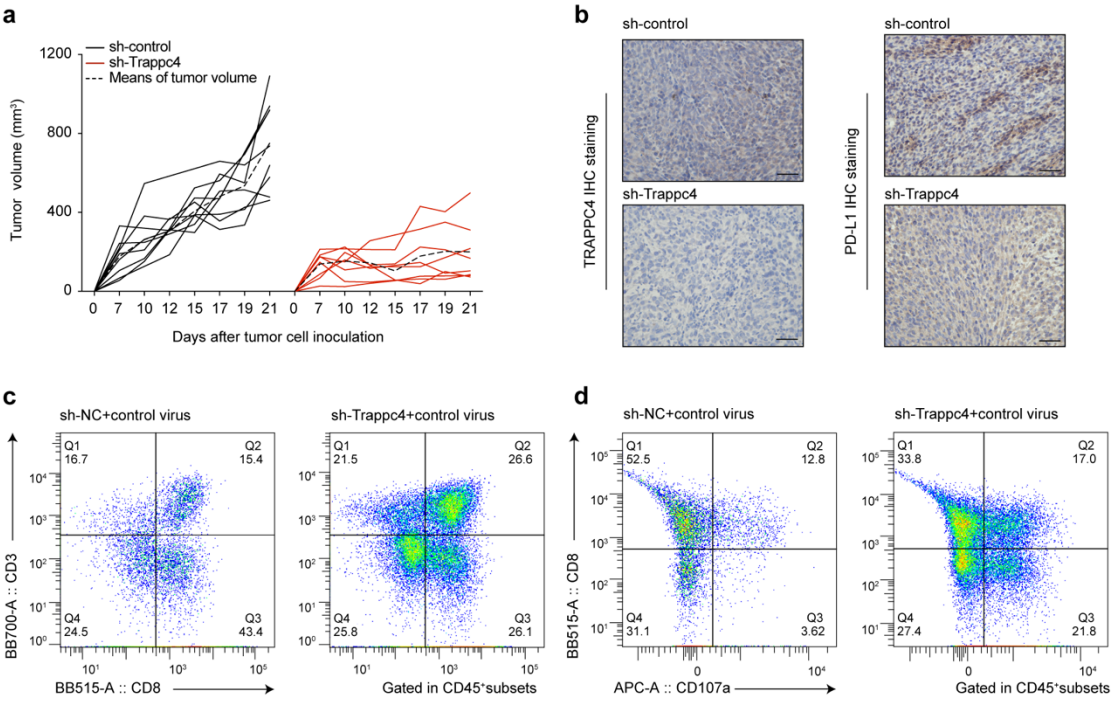

Supplementary Fig. 5 Knockdown of TRAPPC4 affects tumor growth and tumor microenvironment components in vivo. a, The growth of individual tumors in mice bearing control and Trappc4-deficient MC38 tumors (*n*=9 per group). The dashed lines represented the mean volumes of the tumors in the different groups. **b**, Representative immunohistochemical staining of TRAPPC4 and PD-L1 of tumors in different groups of mice. The experiment was repeated in three animal samples with similar results. Scale bars, 100μm. **c& d**, $CD3^+$ $CD8^+$ T cells (c) and $CD8^+$ $CD107a^+$ T cells (d) were analyzed using flow cytometry and the representative images with the percentage of the target subsets are shown, as gated in $CD45^+$ subsets. Source data are provided as a Source Data file.

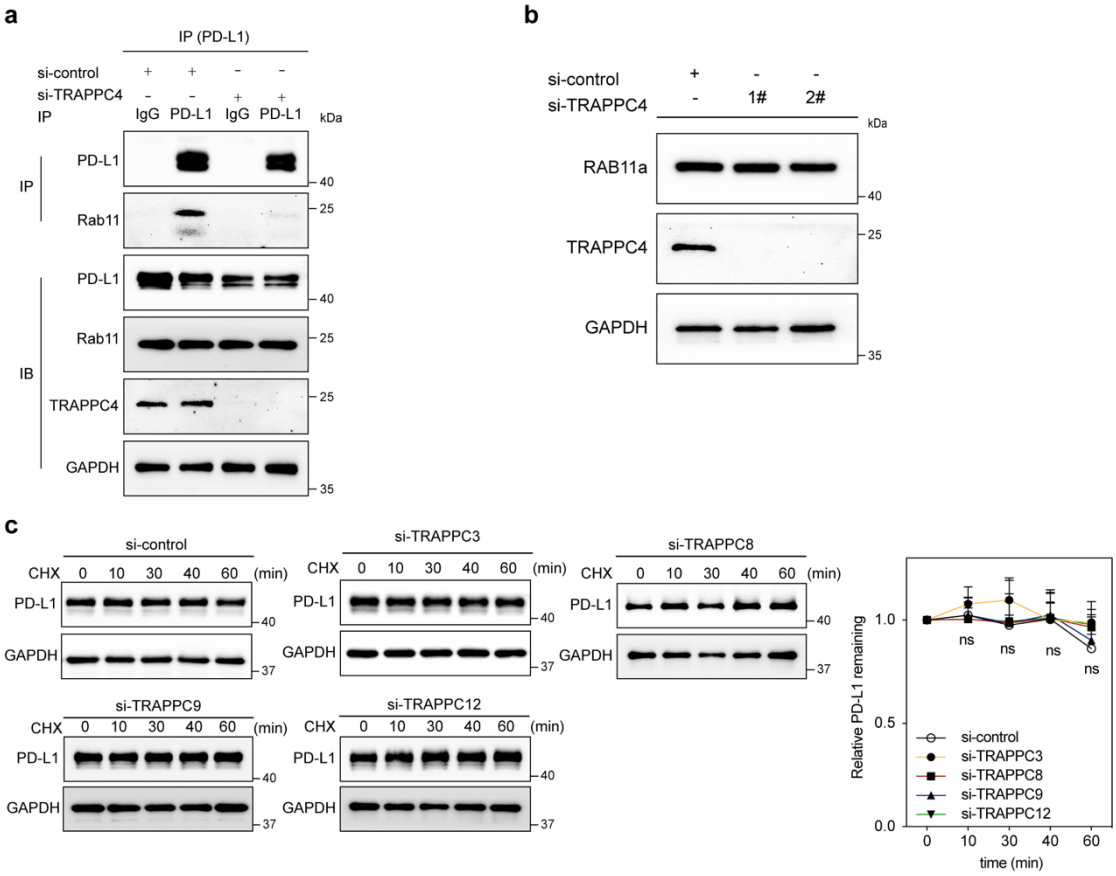

Supplementary Fig. 6 Regulation by TRAPPC4 and RAB11 on the expression of PD-L1. a, The Co-IP assay detecting interaction between PD-L1 and RAB11 with or without the knockdown of TRAPPC4. This experiment was repeated three times with similar results. **b**, Western blotting assay showing that knockdown of Trappc4 did not affect the expression of RAB11 in RKO cells. This experiment was repeated independently three times with similar results. **c**, CHX-chase assay indicating that the stability of PD-L1 was not significantly affected upon the knockdown of the indicated TRAPP subunits in RKO cells. The relative level of the remaining PD-L1 is quantified on the right and values indicates means ± SEM of the relative gray values. Statistical analysis was carried out using a two-tailed Student's *t*-test. This experiment was repeated three times with similar results. ns, not significant. Source data are provided as a Source Data file.

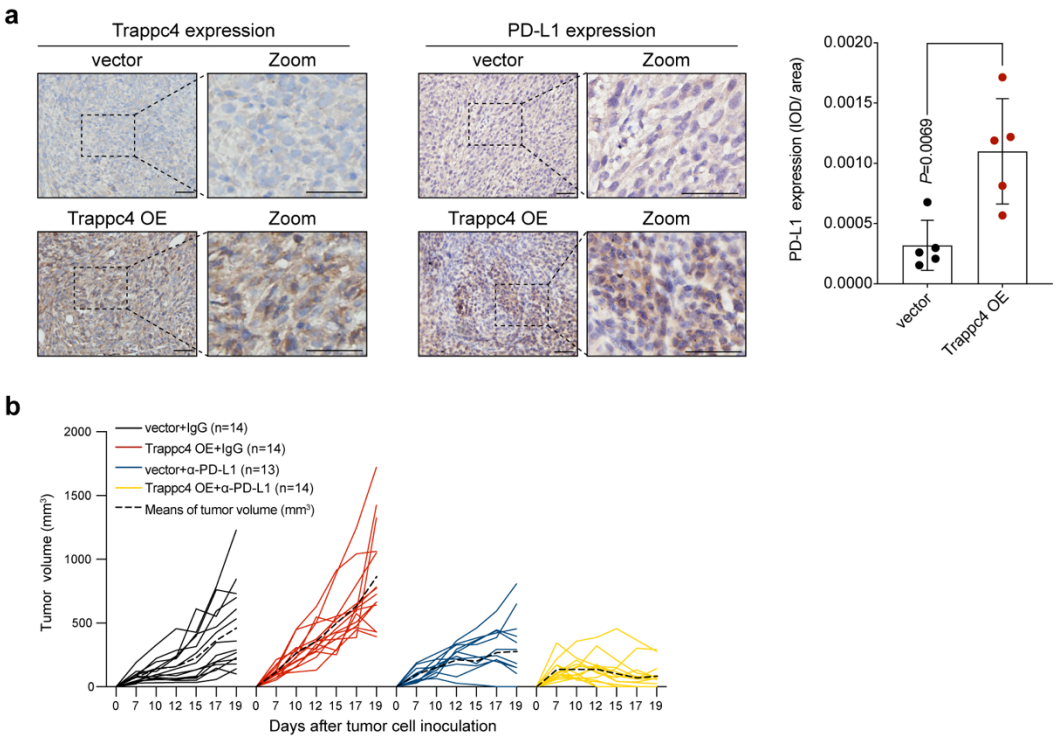

Supplementary Fig. 7 Overexpression of TRAPPC4 promotes the efficacy of immune checkpoint blockade therapy. a, Detection of TRAPPC4 and PD-L1 expression with immunohistochemical staining in control and Trappc4-OE groups. PD-L1 IHC scores were assessed using Image-Pro Plus and values indicates means ± SD from each group (n= 5 per group). Statistical analysis was carried out using a two-tailed Student's t-test. Scale bars, 100 μm. OE, overexpressing. **b**, The growth of individual tumors in the control and Trappc4-OE groups, with or without treatment with the anti-PD-L1 mAb. The dashed lines represent the mean volumes of the tumors in the different groups. Source data are provided as a Source Data file.

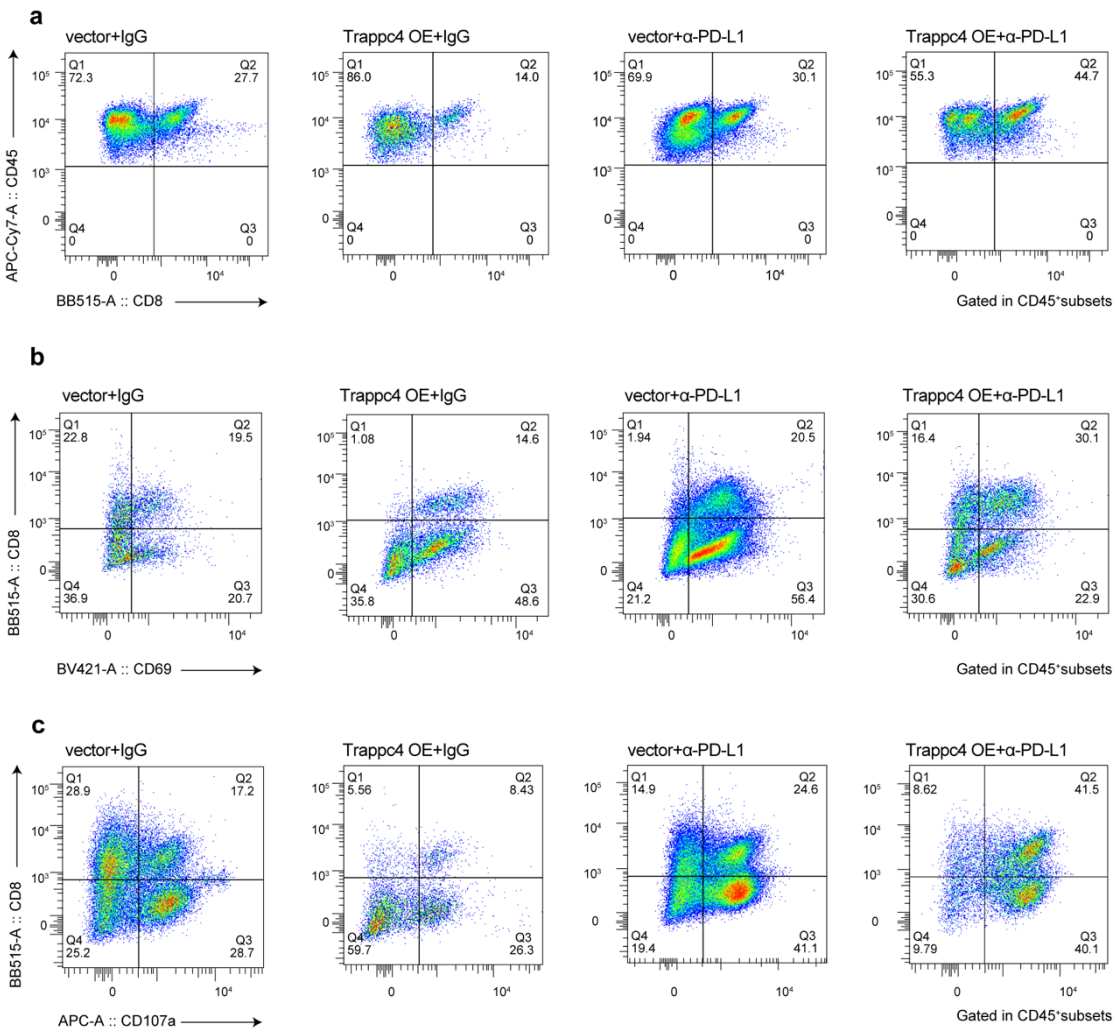

Supplementary Fig. 8 Infiltration of the TILs in Trappc4-OE tumors with or without anti-PD-L1 treatment was analyzed with flow cytometry. a-c, Infiltration of $CD8^+$ T cells (c), $CD8^+$ $C69^+$ T cells (d) $CD8^+$ $CD107a^+$ T cells (e) in different groups in **Fig. 6a** were analyzed using flow cytometry and the representative images with the percentage of the target subsets are shown, as gated in $CD45^+$ subsets. Source data are provided as a Source Data file.

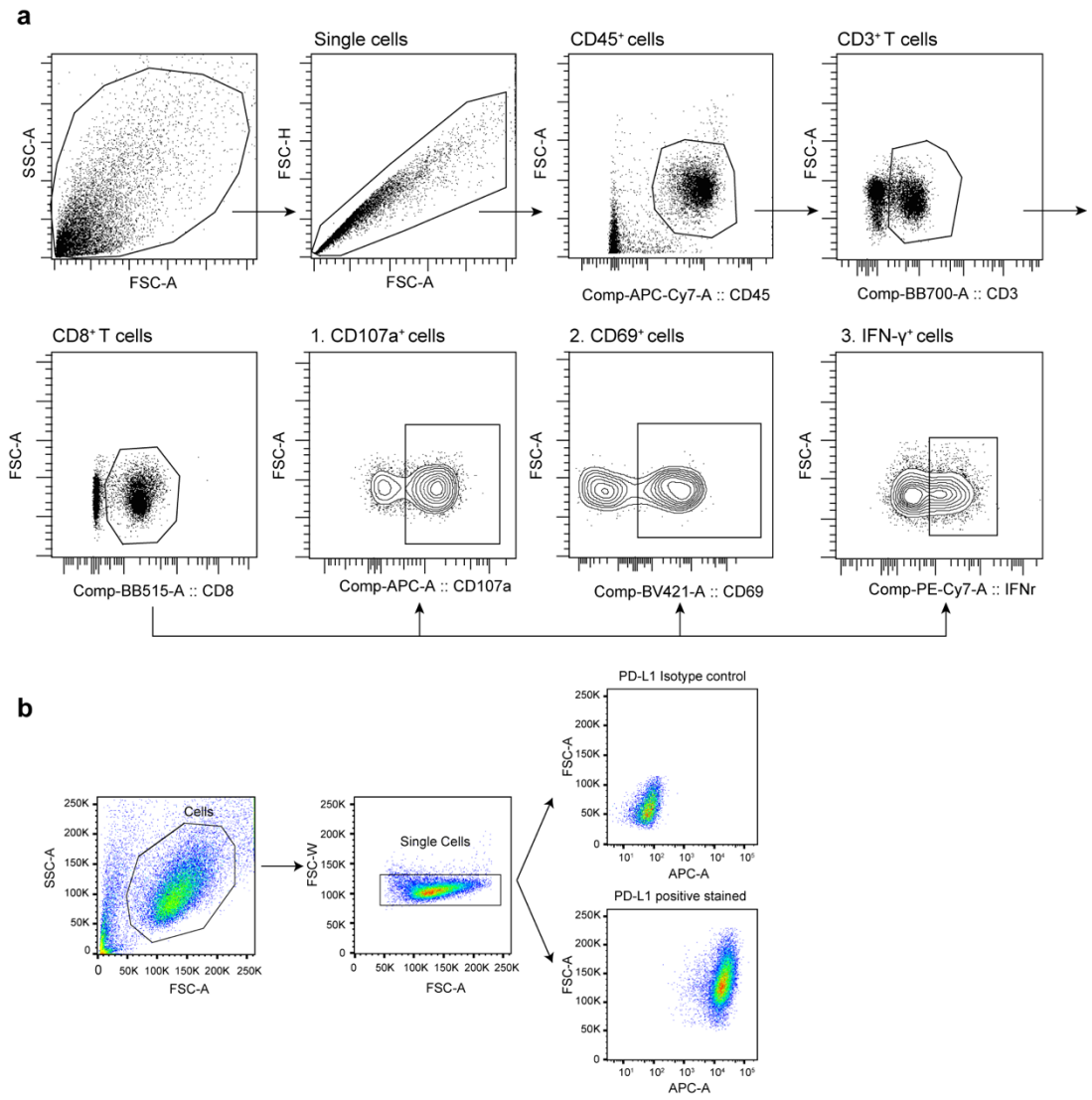

Supplementary Fig. 9 Scheme of the gating strategy used in flow cytometry assays. a, Scheme of the gating strategy used to examine different cell subsets in Fig. 3 and Fig. 6. **b**, Representative example of the gating strategies used for detection of PD-L1 on the cell surface.

Supplementary Tables

Supplementary Table 1. Proteomic analysis of co-expression of PD-L1 and the subunits of TRAPP complex (cohort 2)

Co-expression with PD-L1	Pearson r	*P*-value*
TRAPPC1	0.75	0.09
TRAPPC2	0.00	0.99
TRAPPC3	0.57	0.0045
TRAPPC4	0.69	0.0003
TRAPPC5	0.69	0.0003
TRAPPC6A	-0.05	0.91
TRAPPC6B	0.35	0.1
TRAPPC8	0.41	0.05
TRAPPC9	0.08	0.75
TRAPPC10	0.12	0.61
TRAPPC11	0.23	0.3
TRAPPC12	0.07	0.75
TRAPPC13	0.25	0.27

* Data were analyzed by two-sided Pearson correlation.

Supplementary Table 2. Reagents or resources used in this study

Antibodies			
Name	**Source**	**Catalogue no.**	**Dilution**
Rabbit anti- PD-L1	Cell signaling Technology	CAT#13684	1:1,000 (WB) 1:100 (IHC)
Rabbit anti-PD-L1	Proteintech	CAT#17952-1-AP	1:100 (IF, IHC)
Mouse anti-PD-L1	Cell signaling Technology	CAT#29122	1:100 (IF)
Mouse anti-TRAPPC4	Abcam	CAT#ab57364	1:1,000 (WB)
Mouse anti-TRAPPC4	Abnova	CAT#H00051399-M01	1:1,000 (WB) 1:100 (IF)
Rabbit anti-TRAPPC4	Sigma-Aldrich	CAT#HPA041371	1:1,000 (WB) 1:100 (IHC)
Rabbit anti-CD8	Cell signaling Technology	CAT#98941	1:200
Rabbit anti-CD4	Abcam	CAT#ab183685	1:200
Rabbit anti-Giantin	Abcam	CAT#ab80864	1:200
Rabbit anti-EEA1	Abcam	CAT#ab2900	1:200
Mouse anti-Lamp1	Abcam	CAT#ab25630	1:200
Mouse anti-Rab11	BD Biosciences	CAT#610656	1:1,000

Mouse anti-HA tag	Biolegend	CAT#901513	1:1,000
Anti-GAPDH-HRP	KANGCHENG Technology	CAT#KC-5G5	1:3,000
Anti-rabbit-HRP	KANGCHENG Technology	CAT#KC-RB-035	1:5,000
Anti-mouse-HRP	KANGCHENG Technology	CAT#KC-MM-035	1:5,000
Anti-mouse Alexa Fluor 488 dye conjugated antibody	Invitrogen	CAT#A-21202	1:400
Anti-rabbit Alexa Fluor 594 dye conjugated antibody	Invitrogen	CAT#R37119	1:400
Anti-human Alexa Fluor 488 dye conjugated antibody	Invitrogen	CAT#A-11013	1:400
APC anti-human CD274 (B7-H1, PD-L1) Antibody	Biolegend	CAT#329708	1:250
APC mouse anti-human CD45	BD Biosciences	CAT#561863	1:200
APC-Cy7 Rat anti-mouse CD45	BD Biosciences	CAT#557659	1:100
PerCP Cy5.5 anti-mouse CD3	eBioscience	CAT#45-0031-82	1:100
FITC anti-mouse CD8a	Biolegend	CAT#100706	1:100
BV421 anti-mouse CD69	Biolegend	CAT#104528	1:100
APC anti-mouse CD107a	Biolegend	CAT#121614	1:100
PE-Cy7 Rat anti-mouse IFN-γ	BD Biosciences	CAT#557649	1:50

Chemicals, reagents and Recombinant Proteins		
Name	**Source**	**Catalogue no.**
AOM	Sigma-Aldrich	CAT# A5486
DSS	MP Chemicals Inc	CAT# 0216011080
FuGENE HD	Promega	CAT#E2311
DharmaFECT Transfection Reagent	Dharmacon	CAT#T-2001-02
DharmaFECT Duo Transfection Reagent	Dharmacon	CAT#T-2010-03

Recombinant human PD-1 Fc chimera protein	R&D Systems	CAT#1086-PD-050
Recombinant Human IFN-gamma Protein	R&D Systems	CAT#285-IF-100/CF
Cycloheximide	Sigma-Aldrich	CAT#C1988
Chloroquine	Sigma-Aldrich	CAT#C6628
NH_4Cl	Aladdin Chemistry	CAT#A116373
MG132	Sigma-Aldrich	CAT# M8699
RNAiso Plus	Takara	CAT# 9109
DAPI	SouthernBiotech	CAT#0100-20
Pierce IP Lysis Buffer	Thermo Fisher	CAT#87787
Pierce protein G Agarose	Thermo Fisher	CAT#20398
InVivoMab anti-mouse PD-L1	Bioxcell	CAT#BE0101
Critical Commercial Assays		
Name	**Source**	**Catalogue no.**
FITC Annexin V Apoptosis Detection Kit I	BD Biosciences	CAT#556547
PrimeScript RT Reagent Kit	Takara	CAT# RR036A
TB Green Premix Ex Taq II	Takara	CAT# RR820L
Pierce BCA protein assay kit	Thermo Fisher	CAT#23227
T Cell Activation/Expansion Kit	Miltenyi Biotec	CAT#130-091-441
Recombinant DNA		
Name	**Source**	**Catalogue no.**
pcDNA-Myc-TRAPPC4	GeneRay, Inc	N/A
pcDNA-Flag-PD-L1	GeneRay, Inc	N/A
pcDNA-HA-Rab11	GeneRay, Inc	N/A
pcDNA-HA-Rab11Q70L	GeneRay, Inc	N/A
pcDNA-HA-Rab11S25N	GeneRay, Inc	N/A
Experimental Models: Cell Lines		
Name	**Source**	**Catalogue no.**
HCT116 Cells	ATCC	CAT# CCL-247
RKO Cells	ATCC	CAT# CRL-2577
LoVo Cells	ATCC	CAT# CCL-229
MC38	BMCR	CAT# 1101MOU-PUMC000523
Experimental Models: Strains		
TRAPPC4$^{\Delta IEC}$		N/A
Escherichia coli strain *DH5α*	TIANGEN	CAT#CB101
Biological Samples		

Formalin-fixed paraffin-embedded colorectal cancer tissues	Renji Hospital affiliated with Shanghai Jiaotong University School of Medicine	N/A
Software and Algorithms		
ImageJ 2.1.0	National Institutes of Health (open source)	https://imagej.nih.gov/ij/
Image-Pro Plus 6.0	Media Cybernetics, Inc.	https://www.mediacy.com/imagepro plus
Graphpad Prism 7.03	Graphpad	https://www.graphpad.com/ scientific-software/prism/
ZEN 2011	ZEISS	https://www.zeiss.com/microscopy/
FlowJo 10.4	BD Biosciences	https://www.flowjo.com
FACSDiva 6.2	BD Biosciences	https://www.bdbiosciences.com/en-us/products/software/instrument-software/bd-facsdiva-software

Supplementary Table 3. Clinical and pathological information of 32 cases CRC patients (cohort 1)

NO.	Location	Tumor Size (cm)	Grade	TNM stage	Expression of TRAPPC4 (IOD/area)	Expression of PD-L1 (IOD/area)
1	Descending colon	4*3*0.6	II	T4N1M1	9.57	9.21
2	Sigmoid colon	2.5*1.5*0.8	II	T4N0M0	8.97	8.27
3	Sigmoid colon	4*4*1	II	T3N0M0	4.18	7.30
4	Rectum	4*3.5*1	II	T4aN0M0	11.40	12.45
5	Rectum	5*4*0.8	II	T3N0M0	7.02	4.29
6	Ileocecal junction	5.5*2*1.5	III	T4aN0M0	7.55	3.44
7	Sigmoid colon	4*3.5*0.8	II	T3N1M0	6.24	8.86
8	Ascending colon	4*3*1	II	T3N2M0	3.65	2.94

9	Sigmoid colon	4*3*1	II	T3N0M0	2.97	9.44
10	Ascending colon	5*4*4	II	T3N0M0	6.07	6.58
11	Ileocecal junction	4*4*3	II	T3N0M0	2.64	4.99
12	Rectum	3.5*2*0.5	II	T4aN0M0	3.84	6.98
13	Descending colon	5*5*2.5	II	T4aN0M0	0.03	0.06
14	Transverse colon	6*4*1	II	T3N0M0	12.50	7.29
15	Ileocecal junction	7*7*3	II-III	T3N0M0	14.40	8.78
16	Rectum	3*3*1	II	T4N0M0	12.11	9.15
17	Rectum	5*3.5*1	II	T4N2M0	17.20	24.30
18	Sigmoid colon	7*4*2	II	T4N0M0	9.84	13.31
19	Sigmoid colon	2.5*2*1.2	II	T4N2M1	2.56	0.01
20	Descending colon	6.5*4*3.5	II	T3N0M1	0.00	0.09
21	Ileocecal junction	5*3.5*0.7	II	T3N1M0	0.00	0.11
22	Rectum	5*3*1	II	T4N0M0	3.46	2.74
23	Sigmoid colon	7.5*3.5*3	II	T4N2M1	3.65	3.37
24	Descending colon	3.5*2.5*1	II-III	T4bN1bM0	0.00	0.43
25	Ascending colon	3.5*3*2	II	T3N1aM0	1.43	0.14
26	Rectum	7.5*5*1	II	T3N0M0	0.07	0.06
27	Ascending colon	8*6*1	II	T3N2M1	11.70	15.41
28	Rectum	3.5*1.5*1	II	T4N2M0	10.10	5.04
29	Rectum	7*5.5*2	II	T4N1M0	1.21	1.05
30	Ascending colon	3.5*3*1.5	II	T2N0M0	3.72	2.61
31	Rectum	2.5*2*0.7	II	T2N1M0	0.04	0.23
32	Rectum	4*3*0.5	II	T4N0M0	4.84	4.12

Supplementary Table 4. Sequence of si-RNAs in this study

Target name	Sense (5'-3')	Antisense (5'-3')
TRAPPC4-1	CGCCUCACUUCUAAUGAGATT	UCUCAUUAGAAGUGAGGCGTT
TRAPPC4-2	GGAUCAAGUUUGUGGUUCUTT	AGAACCACAAACUUGAUCCTT
TRAPPC1	GCUCCCGACUGGACUCCUATT	UAGGAGUCCAGUCGGGAGCTT
TRAPPC3	GAGACGGUGUGACAGAAAUTT	AUUUCUGUCACACCGUCUCTT
TRAPPC5	CGCUCAUCAACACCUACAUTT	AUGUAGGUGUUGAUGAGCGTT
TRAPPC6	CGGAUACUGUGUUGUUUGATT	UCAAACAACACAGUAUCCGTT
TRAPPC8	GGGUUGCUAUUUACUUAAATT	UUUAAGUAAAUAGCAACCCTT
TRAPPC9	GGCAUGUGAAACUAUUGAATT	UUCAAUAGUUUCACAUGCCTT
TRAPPC10	CUCCGAAGAUGAUUCACCUTT	AGGUGAAUCAUCUUCGGAGTT
TRAPPC11	GGGCCUGGAUGUAGUUUAUTT	AUAAACUACAUCCAGGCCCTT
TRAPPC12	GAUGCAGUUAAAGACUUGATT	UCAAGUCUUUAACUGCAUCTT
RAB11A-1	GGAGAUUCUGGUGUUGGAATT	UUCCAACACCAGAAUCUCCTT
RAB11A-2	GGAGCUGUAGGUGCCUUAUTT	AUAAGGCACCUACAGCUCCTT
RAB11A-3	CCUAGACUCUACAAAUGUATT	UACAUUUGUAGAGUCUAGGTT

Supplementary Table 5. Primers for quantitative real-time PCR analysis

Gene name	Forward	Reverse
TRAPPC1	TTCCAAACTAGCCGTTACAAACT	GCTCCACATACAGCGCACT
TRAPPC3	ACATTGGAGTCCGGCTGATTG	CCGCAGTTTCCCGAAAGTCAT
TRAPPC4	GTTCCACTCGCTCTTTGCCA	CCAGCTTGCCTAGGATCTGC
TRAPPC5	GTGGGTTTCTCCCCAGTGTAG	TTGAGCGTGCTGTTCTCCTT
TRAPPC8	GAAACCTTTCTTCAGTCGATGCC	ACGCTACCAACATACATGCTAAA
TRAPPC12	CACAGGAGTCGCTGGATAGAC	CTGCTAAGCCTTGCTCCAAAT
PD-L1	TGGCATTTGCTGAACGCATTT	TGCAGCCAGGTCTAATTGTTTT
GAPDH	GCATTGCCCTCAACGACCAC	CCACCACCCTGTTGCTGTAG